ACTA GEOGRAPHICA UNIVERSITATIS COMENIANAE, Vol. 67, 2023, No. 1, pp. 93-113

A COMPARISON AND CO-RELATION BETWEEN ESTIMATED WATER QUALITY PARAMETERS USING BAND RATIO ALGORITHM OF SENTINEL-2 AND LANDSAT 8 DATA AND OBSERVED WATER QUALITY PARAMETERS FOR KAMUZU RESERVOIR OVER LILONGWE RIVER IN MALAWI, AFRICA

Bernard Yamikani Chome[1], Satya Prakash[2]

1 Centre for Applied Systems Analysis (CASA), Lilongwe, Malawi, e-mail: benchome@yahoo.com

2 Sharda University, Greater Noida, India, School of Engineering and Technology, Department of Civil Engineering, e-mail: satya.prakash@sharda.ac.in

Abstract: The evaluation of water quality is essential for effective water resource management. Traditionally, in-situ measurements have been employed to obtain water quality parameters, but in recent times researchers have demonstrated that satellite images offer a reliable tool for estimating water quality parameters. This study focuses on estimating various water quality parameters viz., chlorophyll-a (Chl-a), turbidity, Total Suspended Matter (TSM), Secchi depth, Coloured Dissolved Organic Matter (CDOM), and cyanobacteria in the Kamuzu reservoir of the Lilongwe River for the period 2013-2020 using Sentinel-2 and Landsat 8 satellite imagery. Turbidity and TSM estimates were compared with in-situ data collected during the same period. The comparison revealed favourable R^2 values of 0.9 and 0.69 for TSM and turbidity, respectively, using Sentinel-2 images whereas R^2 values of 0.56 and 0.61 were obtained using Landsat 8 images. The study also generated spatial distribution maps of water quality parameters using both Landsat 8 and Sentinel-2 satellite data which are in good agreement with theoretical expectations for most water quality parameters, except for CDOM and cyanobacteria indicating limitations in estimating these parameters accurately using band ratio algorithms. Nonetheless, this research emphasizes the importance of remote sensing techniques for estimating water quality parameters, potentially serving as a substitute for in-situ data in terms of coverage and frequency, which is a common challenge faced in assessing water bodies worldwide.

Keywords: water quality, remote sensing, Sentinel-2, Landsat 8, TSM, CDOM, Secchi depth, turbidity, chlorophyll-a

1 INTRODUCTION

Water is a very critical resource that ensures economic and developmental growth (Cherif et al., 2019). Water quality is one of the most fundamental aspects of freshwater resources that are studied when it comes to water being supplied to the population for consumption (Potes et al., 2018). Water quality is the measure of chemical, physical and biological parameters for the suitability of water for human and animal consumption as well as for industrial usage (Nyasulu, 2012). Water quality is assessed through different parameters to understand its effect on human and aquatic life health (Stevenson, 1953). Surface and subsurface water quality monitoring is also conducted for a variety of reasons including environmental reporting and research. It is measured by several parameters such as dissolved oxygen, nutrients, turbidity, hardness and phytoplankton etc. (Gholizadeh et al., 2016).

Natural water resources such as rivers and lakes are the major source of water supply to urban cities. Water pollution, all across the globe, has become one of the major problems affecting the water quality (Nyasulu, 2012) of these water resources. Infrastructural development and industrialization are some of the factors leading to the contamination of water resources resulting in poor water quality (Phiri et al., 2005). The key causes of contamination to these natural resources as well as groundwater resources are the ejection of industrial effluents and domestic sewage, which comprises organic pollutants, heavy metals, chemicals and run-off from human activities as well as construction and agriculture (Goldar and Banerjee, 2004). Total Suspended Solids (TSS) is the measure of total organic and inorganic compounds suspended in water while Total Dissolved Solids (TDS) is the measure of total inorganic chemicals including salts and organic compounds dissolved in water (Soomets et al., 2020). Runoff from built environments and effluents leads to an increase in the TSS and TDS which degrade the quality of water (Khan and Ghouri, 2011). Cultivation along the river banks on the other hand leads to runoff rich in nutrients, due to the use of pesticides and fertilizers, which contributes to the formation of algal blooms (Chimwanza et al., 2006) due to the presence of phosphorus and nitrogen in fertilizers (Pereira et al., 2018). Excess quantities of these nutrients lead to a decrease in Dissolved Oxygen (DO) leading to the formation of harmful algae blooms in water bodies.

Water quality is usually calculated through in situ sample collection & measurements and laboratory measurements. These methods have been in use for many years and provide accurate results if proper procedures are followed (Elhag et al., 2019). These methods, however, have their drawbacks. They are laborious, time-consuming, have minimal spatial coverage of water bodies due to access and reach, and the frequency of water sample collection is limited. Sensors have also been deployed in many cases for continuous measurement of water quality parameters but they have their limitations (Sicard et al., 2015). Compared to in situ measurements, satellite images provide large spatial extent and temporal variations of water bodies (Sagan et al., 2020). Depending on the sensor used, satellite images with a short revisit time enable water bodies to be monitored frequently (Bande et al., 2018). Satel-

lite images also help in estimating the water quality of water bodies, not easily accessible (Peppa et al., 2020). Satellite images from Sentinel and Landsat have been used by several authors in monitoring water quality in different parts of the world (Gholizadeh et al., 2016; Bandel et al., 2018; Elhag et al., 2019; Topp et al., 2020; Chen et al., 2020; Kim et al., 2020; Katlane et al., 2020; Shi et al., 2020; Silva et al., 2021).

The primary objective of this study is to assess the effectiveness of using satellite images as an alternative approach for estimating water quality in water bodies, eliminating the need for on-site visits and in-situ water sampling. This methodology has not been extensively explored in the region under study, and given that the Kamuzu reservoir serves as a vital water source for Malawi, it is crucial to monitor its water quality regularly. Due to the inconsistent collection of water samples in previous years, this study can provide valuable insights for authorities to monitor water quality at regular intervals and implement appropriate measures if necessary.

2 STUDY AREA

Lilongwe River runs through Lilongwe, the capital of Malawi, which is experiencing development and a rise in urbanization (Chidya et al., 2016), and a lot of discharge from industrial, domestic, and agricultural activities ends up in this river. The study was conducted on the Lilongwe River in the Lilongwe district of the central region of Malawi to understand the change in the water quality of the dam due to anthropogenic activities. Lilongwe district lies between 14.50 and 13.50 S latitude and between 33.50 and 34.50 E longitude (Figure 1). Dzalanyama mountain range borders the country of Mozambique where the river originates. The river spans a length of approximately 100 km with a catchment area of about 1800 km^2 (Nyasulu, 2012). There are two dams on the Lilongwe River which are used by the Lilongwe Water Board (LWB) for supplying water to the city. These are Kamuzu Dam I (14.170 S and 33.640 E) which was constructed on the Zambezi basin in 1966 and have a capacity of 4,500,000 m^3, and Kamuzu Dam II (14.160 S and 33.680 E) which was constructed in 1989, just below Kamuzu Dam I, and later rehabilitated in 1992, has a capacity of 19,800,000 m^3. Kamuzu Dam I (KD-I) acts as a balancing reservoir and its outflow goes directly into Kamuzu Dam II (KD-II). The reservoir, named Kamuzu Reservoir (Figure 2) was studied for the present work.

Some authors have studied the water quality of the area (Nyasulu, 2012) and its relationship with land use and landcover (Nkwanda et al., 2021), but no study has been conducted to assess the variations in water quality parameters of the reservoir and estimation of water quality parameters using satellite images. In this study, the spatial spread of water quality parameters across the reservoir has been derived using the band ratio algorithm using satellite images and the same has been compared with the in-situ data.

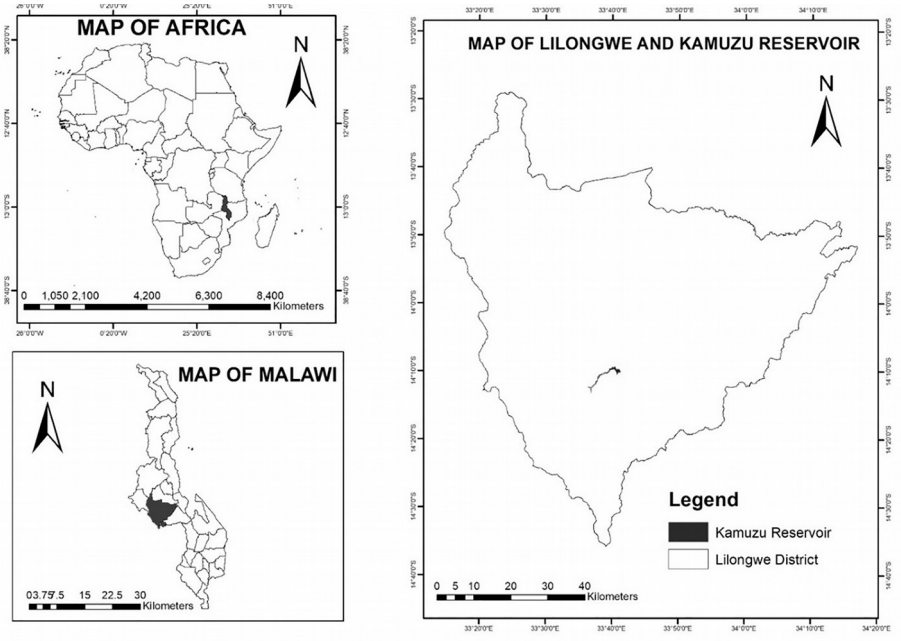

Figure 1 Locator Map of Study Area

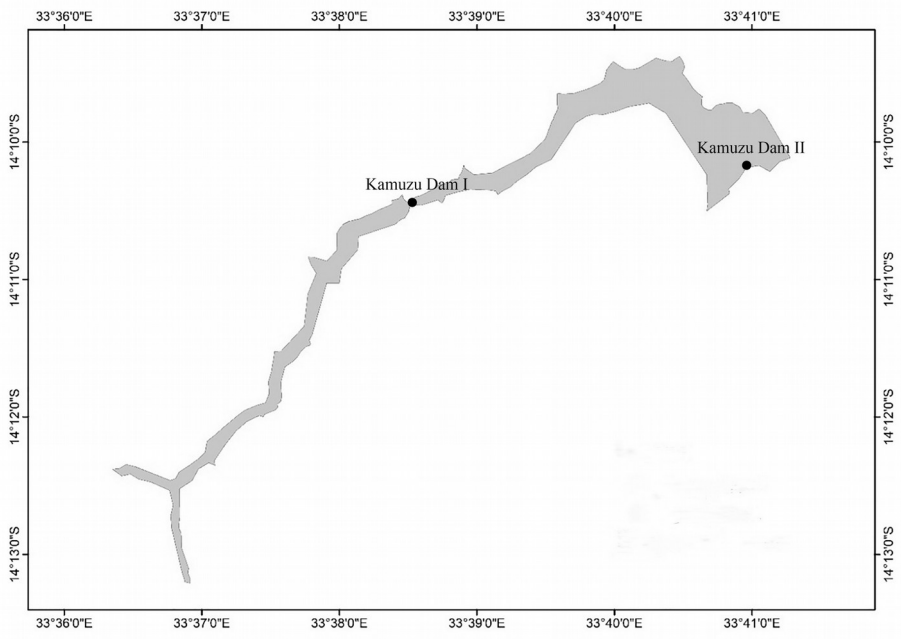

Figure 2 Kamuzu Reservoir along Lilongwe River, Central Malawi, and the location of the Dams

3 MATERIALS AND METHODS

In the present study, the satellite data was used to estimate the water quality parameters which was compared with the in-situ data of the same period. The estimated and in-situ values were further analysed through correlation and regression. The flow chart followed in the study is shown in Figure 3 which shows the different steps followed for the estimation of water quality using different band ratios for Landsat and Sentinel-2 data and its correlation with the in-situ data and the distribution of the water quality parameter in the reservoir. The satellite data (Sentinel-2 and Landsat 8 images) were downloaded from their respective websites (Copernicus https://scihub.copernicus.eu/ for Sentinel-2 and Earth Explorer https://earthexplorer.usgs.gov/ for Landsat 8). Atmospheric correction was applied to the Landsat 8 data, whereas for the Sentinel-2 data no such correction was applied, as it was already corrected for the effects of atmosphere. Both the data sets were clipped using a study-area shapefile to get the image for the study only. Suitable band ratio algorithms (Table 1) were applied to the images to estimate the water quality parameter.

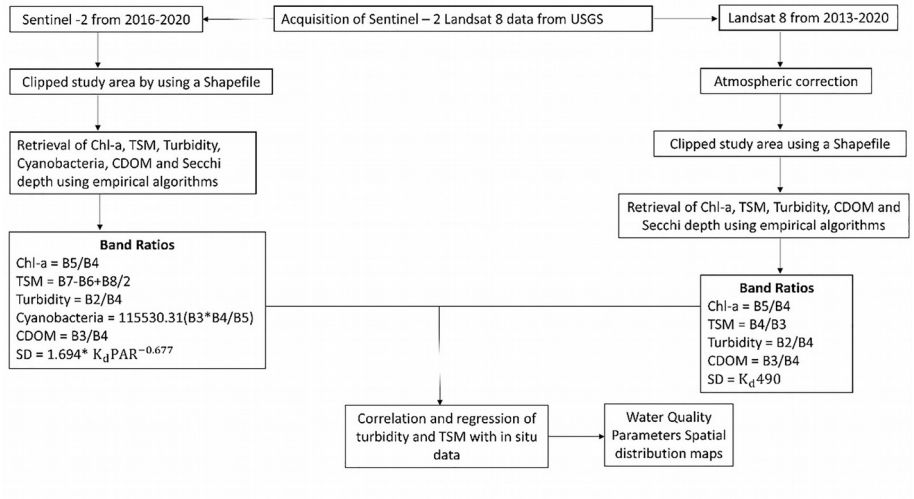

Figure 3 Methodology flowchart showing different steps

The estimated results of water quality parameters from the algorithms were used in a correlation and regression analysis with in-situ data for obtaining the coefficient of determination (R^2). For the values obtained from the processed images to correlate with in situ data, an average pixel value was extracted from a 5×5 pixel window corresponding to the geographical coordinate of the water sampling point. This was necessary to avoid any bias in the estimated values, as a single pixel value may not represent the parameter value correctly.

Table 1 Band ratios used to retrieve Chl-a, TSM, turbidity, CDOM, SD and cyanobacteria from satellite images

Sentinel-2			Landsat 8		
Band ratio	**Water Quality Parameter**	**Reference**	**Band ratio**	**Water Quality Parameter**	**Reference**
R704/R664	Chl-a	(Ansper and Alikas, 2018)	Rrs(NIR)/ Rrs(Red)	Chl-a	(Gholizadeh, *et al*., 2016)
R782-R740+R832/2	TSM	(Soomets *et al*., 2020)	Rrs(Red)/ Rrs(Green)	TSM	(Gholizadeh, *et al*., 2016)
R492/R664	turbidity	(Bande et al., 2018)	Rrs(Blue)/ Rrs(Red)	turbidity	(Bande et al., 2018)
R559/R664	CDOM	(Toming *et al*., 2016)	Rrs(Green)/ Rrs(Red)	CDOM	(Toming *et al*., 2016)
$1.694*K_dPAR^{-0.677}$	SD	(Soomets *et al*., 2020)	K_d490	SD	(Zheng *et al*., 2016)
115530.31*(R559*R 664)/R704	cyanobacteria	(Potes *et al*., 2018)			

For Sentinel-2, R denotes the reflectance and the particular number after R denotes the wavelength. For Landsat 8, Rrs denotes the reflectance and Blue, Green, Red denotes the bands. K_d is the light attenuation coefficient.

3.1 Sentinel-2 MSI data

Sentinel-2, which was launched in 2015, is a European wide-swath, high-resolution, multi-spectral imaging mission. It comprises 2 twin satellites, Sentinel-2A & 2B having a 5-day revisit frequency time. Sentinel-2 carries an optical instrument payload that samples 12 spectral bands: four bands at 10 m (Bands 2, 3, 4 and 8), six bands at 20 m (Bands 5, 6, 7, 8A, 11 and 12) and three bands at 60 m spatial resolution (Bands 1, 9 and 10). Cloud-free Sentinel-2 Level 1C (L1C) MSI data for the study area for the study period has been downloaded which comprises 100 sq. km tiles. A total of 5 cloud-free images (2016-2020) corresponding to the dates of the field sampling (±5 days) were downloaded and processed.

3.2 Landsat 8 data

Landsat 8 is an American Earth Observation Satellite which was launched in 2013 and carries two sensors: the Operational Land Imager (OLI) and the Thermal Infrared Sensor (TIRS). OLI collects data in eight spectral bands (Bands 1-7 and 9) with a spatial resolution of 30 m. Band 8 collects the data with a spatial resolution of 15 m in a panchromatic band. TIRS measures thermal data at 100 m spatial resolution using two bands 10 and 11. Cloud-free Landsat 8 images were downloaded from the United States Geological Survey (USGS). These images were downloaded to match the dates of Lilongwe Water Board field sampling data (±5 days). A total

number of 7 cloud-free (2013-2020) images corresponding to the field sampling dates were downloaded and processed.

3.3 Estimation of water quality parameters using satellite data

Kutser et al. (2016) used the vegetation red edge and NIR in Sentinel-2 to estimate Total Suspended Matter (TSM) and obtained positive results. Gholizadeh et al. (2016) studied many possibilities of band math in Landsat 8 to estimate Chl-a, Secchi depth, Coloured Dissolved Organic Matter (CDOM), Total Suspended Matter (TSM), and turbidity. Potes et al. (2018) used the green and coastal aerosol bands and the green, blue and red bands in Sentinel-2 to map turbidity and cyanobacteria respectively in a reservoir. They concluded that Sentinel-2 had a high potential to monitor turbidity and cyanobacteria. Bresciani et al. (2019) used Sentinel-2 and Landsat 8 to estimate chlorophyll-a, turbidity, and Secchi depth in two reservoirs. They used the Modular Inversion and Processing System to retrieve these parameters. Bande et al. (2018) compared Sentinel-2 and Landsat 8 to generate the effectiveness of one satellite over the other. They estimated the concentration of chlorophyll-a using the coastal aerosol, blue, green and red bands while the blue and red bands were used to estimate turbidity. The results showed that Sentinel-2 had an edge over Landsat 8 data because of its better resolution. Soomets et al. (2020) estimated TSM, Chl-a, Secchi depth, and CDOM from Sentinel-2 data using several band ratio algorithms. They obtained good results after comparison with in-situ data. The various band ratios used for the calculation of the water quality parameters, in the present study are listed in Table 1. These ratios are based on the above studies.

Since the in-situ data were collected between the period of 2013 to 2020, Sentinel-2 satellite data could not be used for the entire study as it is only available from 2016. To correlate the data between 2013-2016, Landsat 8 data was used.

Cloud-free Landsat 8 satellite data of the Kamuzu reservoir were obtained for the period 2013 to 2020 and Sentinel-2 for the period 2016 to 2020. This period matched with the in-situ data collection dates. Landsat 8 images were pre-processed and processed in ERDAS Imagine and SNAP. Band ratio algorithms, as discussed above, were used to estimate the water quality parameters.

The resulting estimated parameters from the satellite images were correlated with in-situ water quality data to validate the results obtained from the satellite images while the other water quality parameters were illustrated as spatial distribution maps.

3.4 In-situ Data

Lilongwe Water Board (LWB) is a Statutory Corporation established in 1947 as a utility service provider and is responsible for the provision of water supply services to the City of Lilongwe and it's surrounding after abstracting raw water from the river through the two dams. The board periodically tests the water for various parameters at the source of the water and treated water. Field sampling data of the

LWB was acquired which consisted of TSM and turbidity measured and the location of the sites from where the samples were collected. The LWB collects the data at 14 different points along the river. Out of the 14 data collection points, only 3 sampling points fall in the study area viz., Katete, Kamuzu Dam I (KD-I), and Kamuzu Dam II (KD-II) as shown in Figure 4. The data ranged from 2013 to 2020, although the frequency of collection was inconsistent. The data obtained from LWB is shown in Table 2.

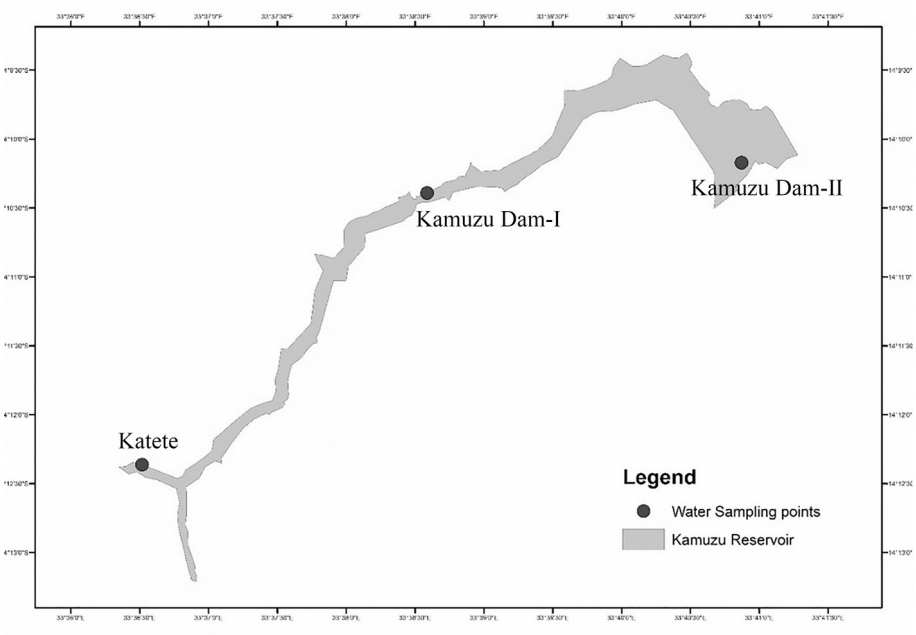

Figure 4 Water Sample points on the study area

The satellite images of the same dates for which the sample was collected were used for processing. However, for days when the cloud-free satellite image for the said date was not available, a few days prior or post the date was selected and the cloud-free image was downloaded and processed for estimation of water quality parameters. Care was taken so that no date of the satellite image is beyond 4 days of the sample collection date. No storm or any other such events have been reported from the region between the date of the sampling date and the date of the satellite image used, the difference in the dates shall not have any effect on the water quality parameter.

Field sampling dates corresponding with satellite imagery dates were also used to perform a correlation and regression analysis. Since only two parameters viz., TSM and turbidity were available for comparison, the correlation and regression analysis of the satellite image estimated TSM and turbidity, with the field-collected

samples of TSM and turbidity were used to determine the coefficient of determination (R^2).

Table 2 In-situ data collected from LWB with name of the stations and the date

	Co-ordinate (UTM)		Date of Sample collection (mm/dd/yyyy)								
Station	Northing (m)	Easting (m)	10/09/2013	04/10/2014	15/06/2016	04/08/2016	12/09/2017	05/07/2018	07/08/2018	09/09/2019	31/10/2019
Katete	564294	8429723	4.81	3.2	1.2	0.4	4	3	3	11	22
Kamuzu Dam I	569230	8432931	12.1	10	2.4	5.2	9	15	4	14	26
Kamuzu Dam II	574129	8433949	3	3.6	5.6	2	10	3	15	10	4

	Co-ordinate (UTM)		Date of Sample collection (mm/dd/yyyy)								
Station	Northing (m)	Easting (m)	10/09/2013	04/10/2014	15/06/2016	04/08/2016	12/09/2017	05/07/2018	07/08/2018	09/09/2019	31/10/2019
Katete	564294	8429723	4.7	2.7	4.7	0.4	3.4	5.3	5.2	8.6	18.7
Kamuzu Dam I	569230	8432931	16.5	6	2.9	3.6	5.1	13.7	7.4	7.9	20.9
Kamuzu Dam II	574129	8433949	4.7	3.2	5.1	1.7	3.3	3.6	5	4.8	3.7

4 RESULTS AND DISCUSSION

The result of the estimated water quality parameter for the study is presented in two parts. The first part describes the spatial distribution of the water quality parameters, as obtained from the satellite images using the band-ratio algorithm. In the second part, the co-relation of the estimated parameters with the in-situ data has been done and the co-relation coefficient has been estimated to see the efficacy of the estimated water quality parameters vis-à-vis in-situ data.

4.1 Spatial distribution of estimated parameters using Sentinel-2 data

The Sentinel-2 satellite data was used to estimate six water quality parameters for the years 2016, 2017 and 2018. Figures 5, 6, and 7 show the spatial distribution of Chl-a, TSM, turbidity, Secchi depth, cyanobacteria and CDOM as estimated using Sentinel-2 images for the years 2016, 2017 and 2018 respectively. Figure 5a shows that there is a high concentration of chlorophyll-a towards the Katete sampling point and some patches of high concentration towards KD-II. According to Gholizadeh et al. (2016) there is a direct relationship between chlorophyll-a and cyanobacteria since cyanobacteria are capable of photosynthesis which needs chloro-

phyll for successful processing. The relationship is evident in Figure 5a and 5e as both the parameters have higher concentration near Katete whereas it decreases for KD-I and KD-II sample points. Figures 5b, 5c, and 5d, show the spread of TSM, Secchi depth, and turbidity. As can be seen that there are some patches of low concentration of TSM (Figure 5b) towards the KD-I and II, and Secchi depth (Figure 5d) is low for the same region whereas turbidity and Secchi depth shows a negative correlation (Figure 5c and 5d). TSM and CDOM usually influence the scattering in the water which is evident from Figure 5b and 5f. CDOM and TSM are in direct correlation as both the values are high near the southern tip of the water body whereas it is uniformly distributed in the northern region. An increase in turbidity relates to less plankton and hence less dissolved oxygen and Chl-a, which is also observed in Figure 5a and 5c.

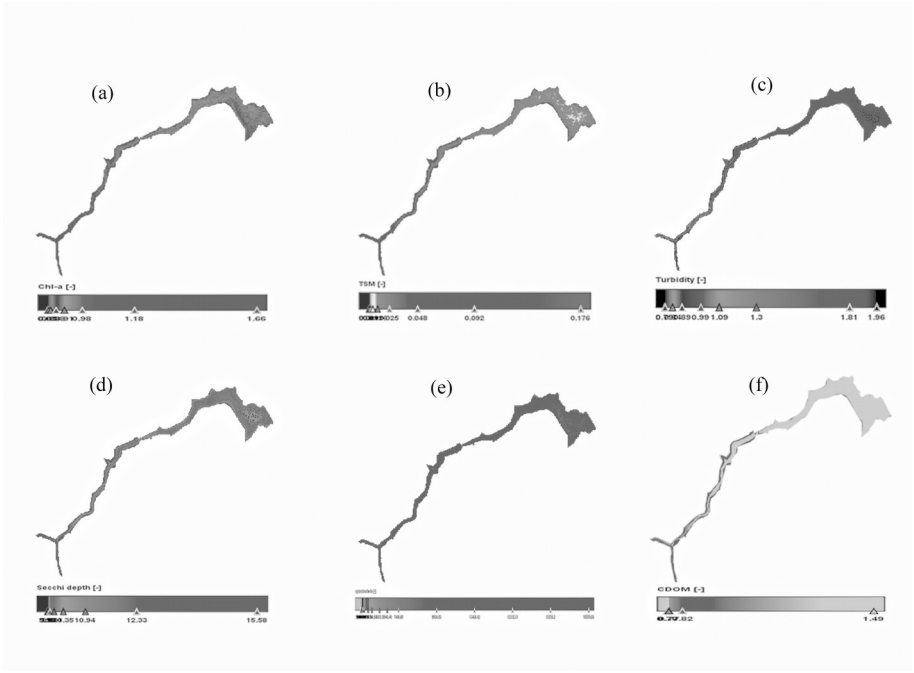

Figure 5 Sentinel-2 spatial distribution maps showing (a) chlorophyll-a, (b) TSM, (c) turbidity, (d) Secchi depth, (e) cyanobacteria, and (f) CDOM for 2nd August 2016

Figures 6a-f shows the spatial distribution of the estimated water quality parameters for 2017 using the Sentinel image of 16th September 2017. The observation is similar to the observation of 2016. As per Figure. 6a, there is a high concentration of chlorophyll-a around the Katete sampling region, but the concentration is low towards KD-II. Figure 6b shows the distribution of Total Suspended Matter and is high in the southern part whereas it reaches a minimum in the northern part near KD-II. The spatial distribution of turbidity is represented in Figure 6c which is al-

most similar and on the mid-high side for the entire study area, except for the northern region where it is maximum. This is also reflected in the Secchi depth spatial distribution in Figure 6d. For most of the region, the values are moderate whereas for the northern region, the values are very less (wherever there is a higher value of turbidity). Cyanobacteria and CDOM distribution are almost uniform throughout the reservoir. Except for Figure 6e and f, all other distribution follows the conventional patterns i.e., wherever there is more turbidity, the Secchi Depth is less representing not-so-clear water, less Chl-a because of less dissolved oxygen and less plankton.

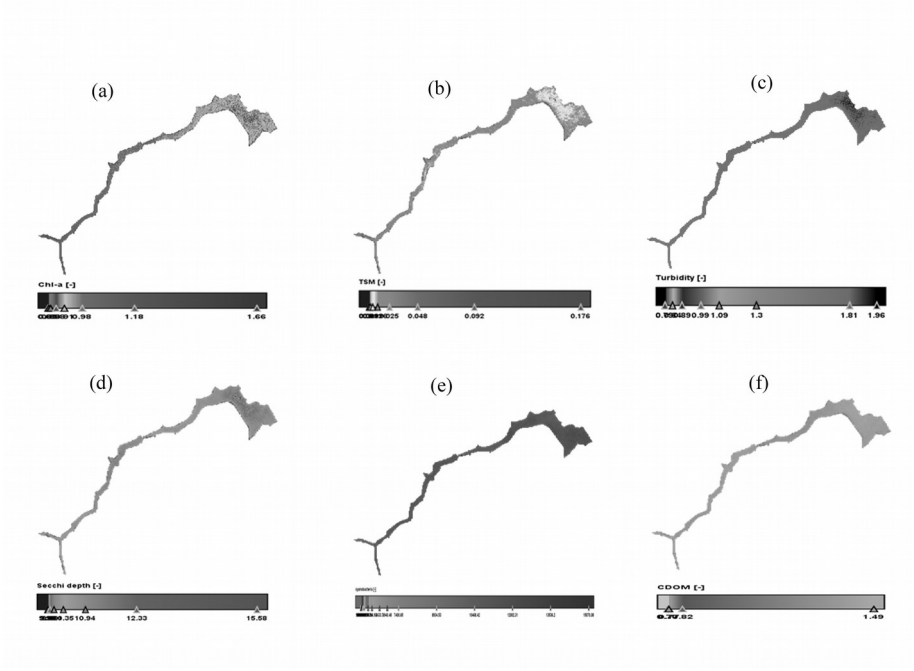

Figure 6 Sentinel 2 spatial distribution maps showing (a) chlorophyll-a, (b) TSM, (c) turbidity, (d) Secchi depth, (e) cyanobacteria, and (f) CDOM for 16th September 2017

The results obtained in Figure 7 for the year 2018 are similar to those in Figure 5 and 6 for years 2016 and 2017 respectively. The relationships observed between water parameters are similar to the earlier years.

The three Sentinel-2 processed figures (Figures 5, 6, and 7) have shown variation in the Chl-a values. The estimated spatial distribution of Chl-a for 2017 and 2018 is almost similar. However, when Chl-a values are compared with 2016, it shows a major change in chlorophyll-a concentration for the KD-II sampling point but almost similar values for Katete and KD-I, which has lower concentrations. The high concentrations of Chl-a are observed from Katete running towards KD-I and are similar for all three years for which the study has been done. The high concentration around Katete and KD-I region can be attributed to the fact that there are settle-

ments and agricultural activities around the region and agricultural and domestic wastes end up in the water leading to high concentrations of Chl-a. The values of Chl-a decrease northwards as there are fewer settlements around the dam area and almost no effluents are passed onto the water body. However, the concentration of Chl-a in 2016 in the northern region was almost similar to that of the southern part, which needs to be studied in more detail.

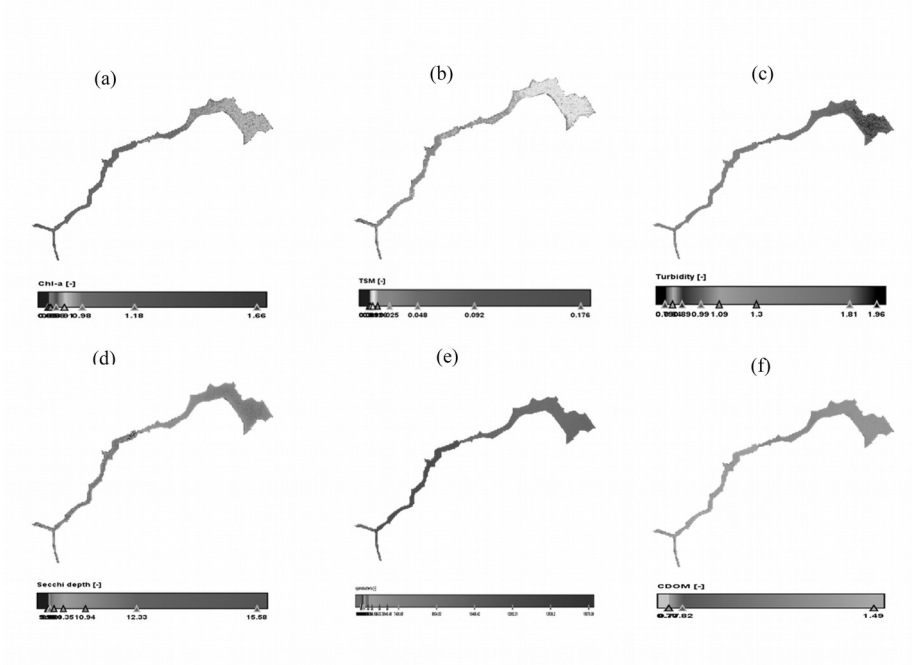

Figure 7 Sentinel-2 spatial distribution maps showing (a) chlorophyll-a, (b) TSM, (c) turbidity, (d) Secchi depth, (e) cyanobacteria, and (f) CDOM for 3rd July 2018

The Figures 5-10 also show the relationship that is there between Secchi depth, turbidity, and TSM. All the figures show a direct relationship between Secchi depth and TSM while there is an inverse relationship between Secchi depth and turbidity. The depth of water transparency is low towards the KD-II compared to the KD-I and Katete sampling regions, at the same time TSM concentration is low while turbidity concentration is high.

4.2 Spatial distribution of estimated parameters using Landsat data

Landsat 8 satellite data was used to estimate five water quality parameters for the years 2013, 2014 and 2019. Figures 8, 9, and 10 show the spatial distributions of Chl-a, TSM, turbidity, Secchi depth and CDOM, as estimated from the Landsat 8

data. The spatial distribution of these parameters for all the years is almost similar as can be observed in the figures. The Chl-a distribution indicates a high concentration towards the Katete sampling region but has a low concentration towards the KD-I & II. CDOM distribution shows a low concentration near Katete which increases towards KD-I and increases further towards KD-II and remains almost uniform near KD-II. Turbidity and Secchi depth distribution show an inverse relationship, which is expected, and turbidity increases from Katete to KD-I and further towards KD-II and corresponding Secchi depth decreases from Katete towards KD-I and further to KD-II. TSM and turbidity also follow an inverse relationship for the region between Katete and KD-I, however, for the area around KD-II, the turbidity has a very high value, but the TSM does not vary accordingly. There are some patches in the area around KD-II where the TSM varies from moderate to low which is also reflected similarly in the distribution of Secchi depth. A few patches of low concentration of TSM and Secchi depth near the KD-II sampling point need to be investigated more, as all other parameters are distributed as expected.

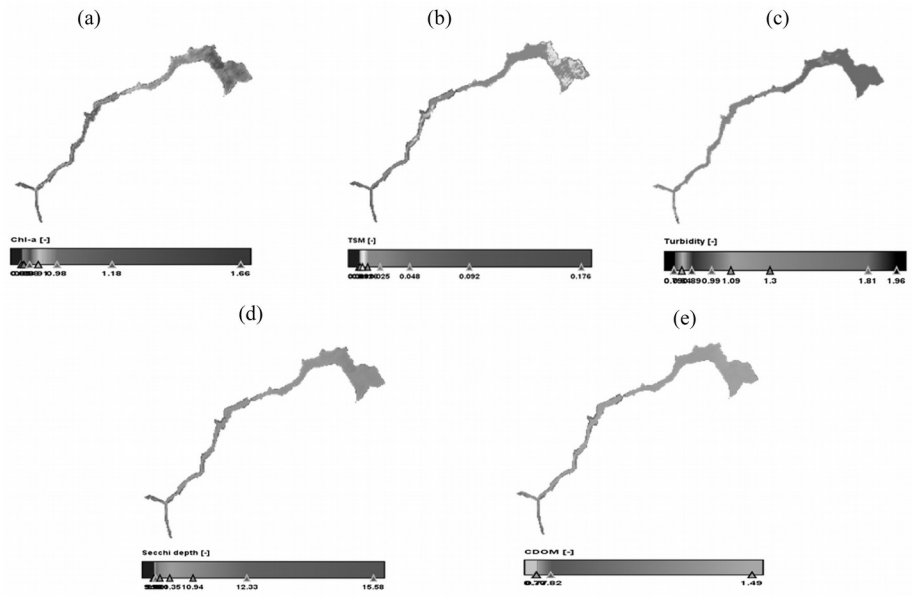

Figure 8 Landsat 8 spatial distribution maps showing (a) chlorophyll-a, (b) TSM, (c) turbidity, (d) Secchi depth, and (e) CDOM for September 2013

Comparing the results of parameters between the time series, the Chl-a is almost similar for Katete between 2013, 2014 and 2019. However, the value increases in 2014 from 2013 and then decreases in 2019. CDOM values for all the years are similar for all the observation stations and are more or less uniform over the period. Turbidity is least at Katete station for all the years but has increased over time. For KD-I, the turbidity increases as compared to Katete and further increases around the

observation point KD-II. Turbidity in the northern region near KD-II is maximum for all the years but decreases in 2014 as compared to 2013 but again increases in 2019. For all the years, Secchi depth is inversely related to turbidity and the same is the case with TSM.

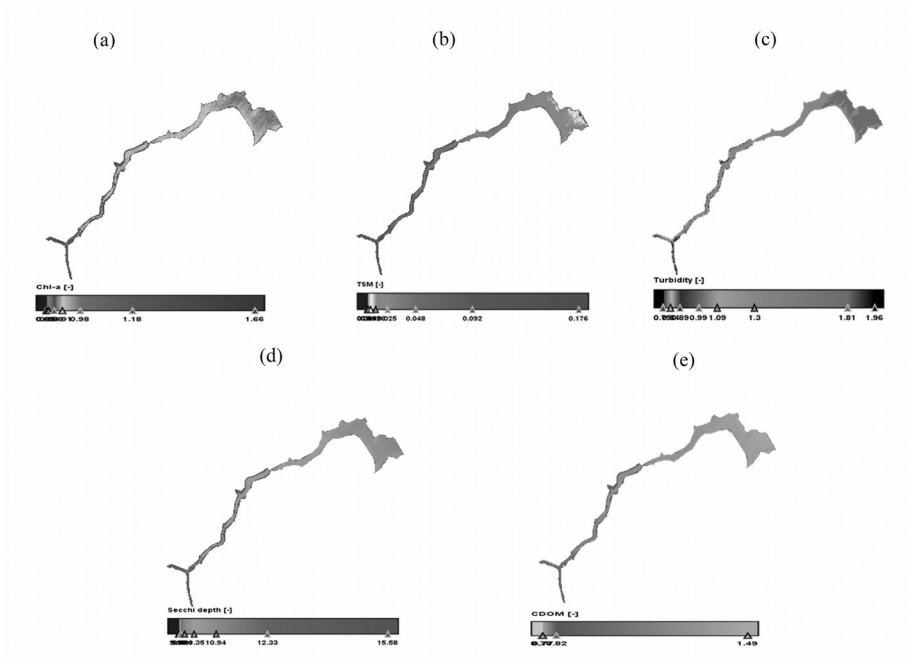

Figure 9 Landsat 8 spatial distribution maps showing (a) chlorophyll-a, (b) TSM, (c) turbidity, (d) Secchi depth, and (e) CDOM for October 2014

4.3 Validation of the estimated data vs in-situ data using correlation and regression analysis

As stated earlier, only two data viz., turbidity and TSM were common between the estimated and in-situ data collected for the study area during the study period. A correlation and regression analysis was performed between the two data to understand the efficacy of the satellite image-derived water quality parameters and whether these could replace the manual and tedious data collection procedure. In-situ data were available for 3 sampling points over a period resulting in 15-20 data points to be validated depending upon the availability of the cloud-free satellite data. For all the sample points the TSM and turbidity values were read from the satellite-generated TSM and turbidity spatial distribution maps (Figures 5-10). Since these estimated data were found using band-ratio algorithms, the resultant values were dimensionless. A co-relation graph between the observed and estimated values was plotted, as shown in Figure 11.

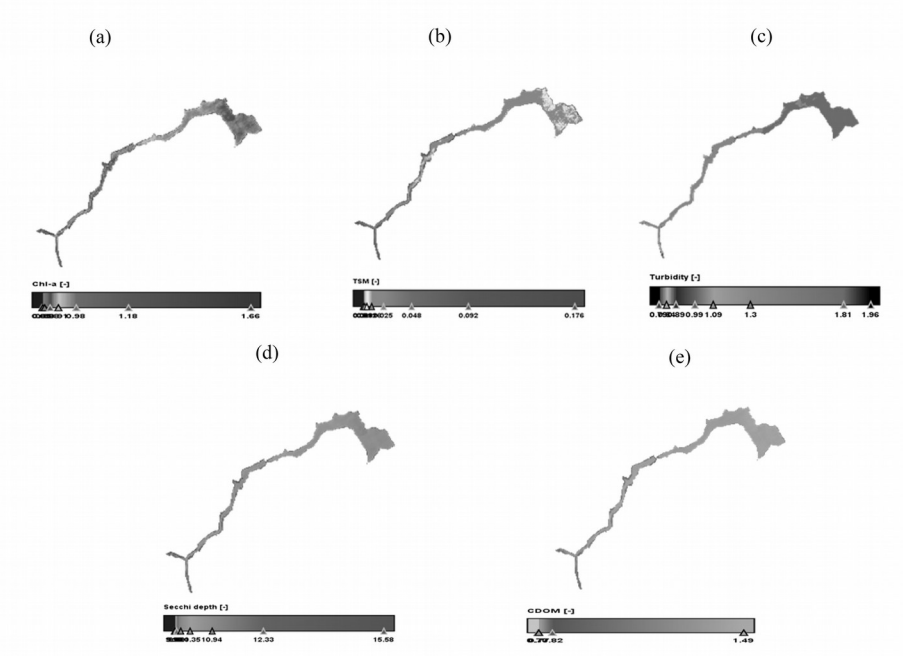

Figure 10 Landsat 8 spatial distribution maps showing (a) chlorophyll-a, (b) TSM, (c) Turbidity, (d) Secchi depth, and (e) CDOM for September 2019

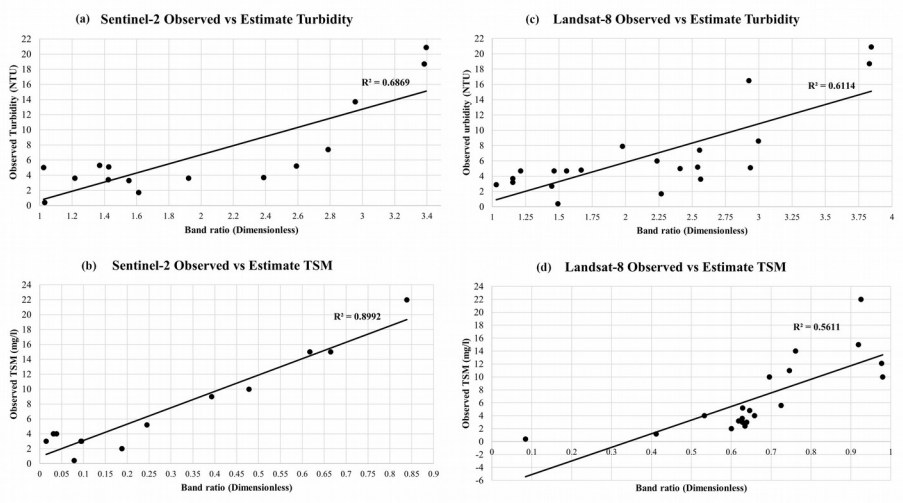

Figure 11 Co-relation graph between observed and estimated values of TSM and turbidity for Landsat 8 and Sentinel-2 satellite data

Figure 11a and Fibure 11b are the co-relation curve for Sentinel-2 data vis-à-vis observed values as obtained by field sampling whereas Figure 11c and Fibure 11d are that of Landsat 8. It was observed that the co-relation coefficient of TSM is 0.9 (Figure 11b) and that of turbidity is 0.7 (Figure 11a). The same for Landsat 8 was found to be 0.6 (Figure 11c) and 0.56 (Figure 11d) respectively. As the turbidity and TSM values show a strong co-relation for Sentinel-2 data as compared to the Landsat 8 data, the same may be used to estimate the TSM and turbidity values to a reasonable accuracy. However, the number of sample points was less, nonetheless, it can be concluded that Sentinel-2 satellite data and band-ratio algorithms can be used to fairly estimate the water quality parameters for a large water body as has also been reported by several other studies. The better accuracy of Sentinel-2 is a result of the better spatial resolution of the satellite data than the Landsat 8 data. Since the observed samples over the years were not tested for other parameters and hence the estimated values could not be compared, a fair assessment of the parameters can be done using satellite data. The observed and estimated values of the two parameters for both Sentinel-2 and Landsat are compiled in Table 3.

The variation in the estimated data for some of the parameters at a few locations may be attributed to the fact that the water body under study is a fairly large water body and the samples were taken only from the banks of the river and the dam, whereas the satellite data used in the study was of 10 m and 30 m spatial resolution spread over the entire dam. Better spatial resolution such as 5 m or 1m satellite data may result in better estimation of the water quality parameters.

5 CONCLUSION

Remote sensing offers an effective solution to address some of the challenges encountered in water quality monitoring. By conducting a correlation analysis between Total Suspended Matter (TSM) and turbidity derived from Sentinel-2 satellite imagery and comparing it with in-situ data, it has been observed that reliable precision can be achieved in estimating turbidity and TSM using satellite images. The findings indicate that Sentinel-2 outperforms Landsat 8 in estimating these parameters due to its superior spatial resolution. Consequently, it can also be concluded that remote sensing data plays a vital role in facilitating effective water quality monitoring.

Furthermore, the results demonstrate the significant potential of Sentinel-2 and Landsat 8 data in estimating various water quality parameters such as chlorophyll-a (Chl-a), TSM, turbidity, cyanobacteria, CDOM concentrations, and Secchi Depth through band ratio algorithms. This enables the estimation and assessment of water quality on a broader spatial scale through the creation of distribution maps. The study also highlights the capability of remote sensing to overcome the limitations of in-situ data availability, particularly regarding the infrequent sampling frequency over seven years. Sentinel-2 and Landsat 8, with their short revisit times of 5 and 16 days respectively, offer a solution to this problem.

Table 3 Comparison between in-situ and satellite-based estimated values

TSM (mg/l) using Sentinel-2 data		
Band Ratio	**Observed TSM (mg/l)**	**Estimated (mg/l)**
0.839	22	19.3
0.665	15	15.5
0.6174	15	14.5
0.478	10	11.4
0.393	9	9.5
0.245	5.2	6.3
0.188	2	5.0
0.0945	3	3.0
0.0387	4	1.8
0.03245	4	1.6
0.0312	4	1.6
0.0147	3	1.2
0.0955	3	3.0
0.07855	0.4	2.6
0.188	2	5.0

Turbidity (NTU) using Sentinel-2 data		
Band Ratio	**Turbidity (NTU)**	**Estimated (NTU)**
2.38741	3.7	9.0
2.78692	7.4	11.4
3.38351	18.7	15.1
3.39559	20.9	15.1
2.95602	13.7	12.5
2.59058	5.2	10.3
1.6134	1.7	4.4
1.92245	3.6	6.2
1.5526	3.3	4.0
1.42522	3.4	3.2
1.42797	5.1	3.2
1.3705	5.3	2.9
1.02439	5	0.8
1.21774	3.6	2.0
1.0311	0.4	0.9

TSM (mg/l) from Landsat 8 data		
Band Ratio	**Observed TSM (mg/l)**	**Estimated (NTU)**
0.60014	2	5.4
0.97948	10	13.4
0.97677	12.1	13.4
0.65855	4	6.7
0.7251	5.6	8.1
0.91895	15	12.2
0.9254	22	12.3
0.76144	14	8.8
0.63851	3	6.2
0.6958	10	7.5
0.41187	1.2	1.5
0.63446	2.4	6.2

Turbidity (NTU) from Landsat 8 data		
Band ratio	**Turbidity (NTU)**	**Estimated (NTU)**
1.15363	3.2	1.5
1.5567	4.7	3.6
2.99668	8.6	10.8
3.82953	18.7	15.0
3.84342	20.9	15.1
2.55437	7.4	8.6
2.93637	5.1	10.5
2.26803	1.7	7.2
2.54111	5.2	8.5
2.56268	3.6	8.6
1.97594	7.9	5.7
2.92536	16.5	10.5

	0.61871	3.2	5.8		2.23547	6	7.0
	0.084511	0.4	-5.4		2.40942	5	7.9
	0.62848	5.2	6.0		1.66672	4.8	4.1
	0.62753	3.6	6.0		1.463	4.7	3.1
	0.6463	4.81	6.4		1.44535	2.7	3.0
	0.74577	11	8.5		1.21165	4.7	1.8
	0.53297	4	4.0		1.15388	3.7	1.5
	0.6958	10	7.5		1.02939	2.9	0.9
	0.62819	3	6.0		1.49234	0.4	3.2

The study further reveals that the upstream region from Katete to Kamuzu Dam I exhibits the highest concentrations of all water parameters in the reservoir compared to the region between Kamuzu Dam I and Kamuzu Dam II. This region coincides with the high population density and numerous anthropogenic activities, predominantly farming. Consequently, the reservoir acts as a receptor for agricultural effluents washed off by runoff in this area.

The authors conducted offline processing of downloaded satellite images, which proved time-consuming. However, the availability of historical and current satellite data, along with processing tools offered by the Google Earth Engine (GEE) platform, has simplified and expedited water quality assessments. For a comprehensive understanding of the seasonal variation of water quality parameters and their relationship with anthropogenic activities in the region, future studies could utilize GEE to analyze the evolving water quality of the reservoir.

Acknowledgements

The authors express their gratitude to Mr Charles Kachingwe, the Water Quality Officer at Lilongwe Water Board (LWB), Malawi, for his invaluable assistance in acquiring the in-situ data and granting permission to utilize the data for this research paper. Additionally, BC would like to extend thanks to the Government of Malawi for sponsoring his post-graduate program at Sharda University, during which this study was conducted. SP acknowledges the University for providing the essential facilities that contributed to the completion of this research. The authors would also like to express their appreciation to the anonymous reviewer for his constructive feedback, which has significantly improved the manuscript.

References

ANSPER, A., ALIKAS, K. 2018. Retrieval of Chlorophyll a from Sentinel-2 MSI Data for the European Union Water Framework Directive Reporting Purposes. *Remote Sensing*, 11, 64-68.

BANDE, P., ADAM, E., ELBASIT, M., ADELABU, S. 2018. Comparing Landsat 8 and sentinel-2 in mapping water Quality at Vaal Dam. In *IEEE conference IGRASS 2018*.

BRESCIANI, M., GIARDINO, C., STROPPIANA, D., DESSENA, M. A., BUSCARINU, P., CABRAS, L., SCHENK, K., HEEGE, T., BERNET, H., BAZDANIS, G., TZIMAS, A. 2019. Monitoring water quality in two dammed reservoirs from multispectral satellite data. *European Journal of Remote Sensing*, 52, 113-122.

CHEN, J., ZHANG, D., YANG, S., NANEHKARAN, Y. A. 2020. Intelligent monitoring method of water quality based on image processing and RVFL-GMDH model. *IET Image Process*, 14, 4646-4656.

CHERIF, E. K., SALMOUN, F., MESAS-CARRASCOSA, F. J. 2019. Determination of Bathing Water Quality Using Thermal Images Landsat 8 on the West Coast of Tangier: Preliminary Results. *Remote Sensing*, 11, 972-980.

CHIDYA, R. C., MULWAFU, W. O., BANDA, S. C. 2016. Water supply dynamics and quality of alternative water sources in low-income areas of Lilongwe City, Malawi. *Physics and Chemistry of the Earth*, 93, 63-75.

CHIMWANZA, B., MUMBA, P. P., MOYO, B. H. Z., KADEWA, W. 2006. The impact of farming on river banks on water quality of the rivers. *International Journal of Environmental Science and Technology*, 2, 4, 353-358.

ELHAG, M., GITAS, I., OTHMAN, A., BAHRAWI, J., GIKAS, P. 2019. Assessment of Water Quality Parameters Using Temporal Remote Sensing Spectral Reflectance in Arid Environments, Saudi Arabia. *Water*, 11, 1-14.

GHOLIZADEH, M., MELESSE, A., REDDI, L. 2016. A Comprehensive Review on Water Quality Parameters Estimation Using Remote Sensing Techniques. *Sensors*, 16, 1298.

GOLDAR, B., BANERJEE, N. 2004. Impact of informal regulation of pollution on water quality in rivers in India. *Journal of Environmental Management*, 73, 117-130.

KATLANE, R., DUPOUY, C., BERGÉS, J.-C., MANNAI, A. 2020. Estimation of Chl-a conc in estuarine water of Kneiss Archpileago Gulf of Gabes using Sentinel-2A and EO1 data. In *IEEE Conference M2GRASS 2020*.

KHAN, M., A., GHOURI, A. M. 2011. Environmental Pollution: Its Effects on Life and Its Remedies. *Researcher World: Journal of Arts, Science & Commerce*, 2, 276-28. [online] [cit. 2023-05-30]. Available at: <https://ssrn.com/abstract=1981242>

KIM, Y. H., SON, S., KIM, H.-CH., KIM, B., PARK, Y.-G., NAM, J., RYU, J. 2020. Application of satellite remote sensing in monitoring dissolved oxygen variabilities: A case study for coastal waters in Korea Application of Sentinel 2 MSI Images to Retrieve Suspended Particulate Matter Concentrations in Poyang Lake. *Environment International*, 134, 1-10.

KUTSER, T., CASAL, G., BARBOSA, C., PAAVEL, B., FERREIRA, R., CARVALHO, L., TOMING, K. 2016. Mapping inland water carbon content with Landsat 8 data. *International Journal of Remote Sensing*, 373, 2950-2961.

NKWANDA, I. S., FEYISA, G. L., ZEWGE, F., MAKWINJA, R. 2021. Impact of land-use/land-cover dynamics on water quality in the Upper Lilongwe River basin, Malawi. *International Journal of Energy and Water Resources*, 5, 193-204.

NYASULU, T. H. 2012. *Assessment of the Quality of Water in Urban Rivers-A case study of Lilongwe River in Malawi*. Unpublished MS thesis. [online] [cit. 2023-05-30]. Available at: <https://catalog.ihsn.org/index.php/citations/33290>

PEPPA, M., VASILAKOS, C., KAVROUDAKIS, D. 2020. Eutrophication Monitoring for Lake Pamvotis, Greece, Using Sentinel-2 Data. *ISPRS International Journal of Geo-Information*, 9, 143-156.

PEREIRA, L. S. F., ANDES, L. C., COX, A. L., GHULAM, A. 2018. Measuring Suspended-Sediment Concentration and Turbidity in the Middle Mississippi and Lower Missouri Rivers Using Landsat Data. *JAWRA Journal of the American Water Resources Association*, 54, 440-450.

PHIRI, O., MUMBA, P., MOYO, B. H. Z., KADEWA, W. 2005. Assessment of the impact of industrial effluents on water quality of receiving rivers in urban areas of Malawi. *International Journal of Environmental Science & Technology*, 2, 237-244.

POTES, M., RODRIGUES, G., PENHA, A. M., NOVAIS, M. H., COSTA, M. J., SALGADO, R., MORAIS, M. M. 2018. Use of Sentinel 2 – MSI for water quality monitoring at Alqueva reservoir, Portugal. P*roceedings of the International Association of Hydrological Sciences*, 380, 73-79.

SAGAN, V., PETERSON, K., MAIMAITIJIANG, M., SIDIKE, P., SLOAN, J., GREELING, B., MAALOUF, S., ADAMS, C. 2020. Monitoring inland water quality using remote sensing: potential and limitations of spectral indices, bio-optical simulations, machine learning, and cloud computing. *Earth-Science Reviews*, 205, 103187-103204.

SHI, K., ZHANG, YU., ZHANG, YI., QIN, B., ZHU, G. 2020. Understanding the long-term trend of particulate phosphorus in a cyanobacteria-dominated lake using MODIS-Aqua observations. *Science of the Total Environment*, 737, 139736-139751.

SICARD, C., GLEN, C., AUBIE, B., WALLACE, D., JAHANSHAHI-ANBUHI, S., PENNINGS, K., DAIGGER, G. T., PELTON, R., BRENNAN, J. D., FILIPE, C. D. M. 2015. Tools for water quality monitoring and mapping using paper-based sensors and cell phones. *Water Research*, 70, 360-369.

SILVA, M. G. G., SILVA, D. J., COSTA, P. D., SILVA, R. C., CASSIMIRO, T. E. B., AMORIM, L. S., ROCHA, D. A., PEIXOTO, Z. M. A. 2021. Analysis of water quality at hydrographic basin scale using satellite images, co-occurrence matrices and Bayes classifier. *Water Supply*, 21, 4418-4428.

SOOMETS, T., UUDEBERG, K, JAKOVELS, D., BRAUNS, A., ZAGARS, M., KUTSER, T. 2020. Validation and Comparison of Water Quality Products in Baltic Lakes Using Sentinel-2 MSI and Sentinel-3 OLCI Data. *Sensors*, 20, 742-753.

STEVENSON, A. H. 1953. Studies of Bathing Water Quality and Health. *American Journal of Public Health and the Nations Health*, 43, 529-538.

TOMING, K., TIIT K., ALO L., MARGOT S., BIRGOT P., TIINA N. 2016. First Experiences in Mapping Lake Water Quality Parameters with Sentinel-2 MSI Imagery. *Remote Sensing*, 8, 8, 640-655.

TOPP, S. N., PAVELSKY, T. M., JENSEN, D., SIMARD, M., ROSS, M. R. V. 2020. Research Trends in the Use of Remote Sensing for Inland Water Quality Science: Moving Towards Multidisciplinary Applications. *Water*, 12 169-183.

ZHENG, Z., REN, J., LI, Y., HUANG, C., LIU, GE, DU, C., LYU, H. 2016. Remote sensing of diffuse attenuation coefficient patterns from Landsat 8 OLI imagery of turbid inland waters: A case study of Dongting Lake. *Science of The Total Environment*, 573, 39-54.

Porovnanie a vzťah medzi odhadovanými parametrami kvality vody použitím algoritmu údajov Sentinel-2 a Landsat 8 a pozorovanými parametrami na príklade vodnej nádrže Kamuzu na rieke Lilongwe v Malawi

Súhrn

Príspevok bol zameraný na vyhodnotenie účinnosti satelitného snímkovania pri odhadovaní parametrov kvality vody, čím sa eliminuje potreba návštev a odberu vzoriek vody na mieste. V úvode sa v článku diskutuje o rôznych metódach používaných na výpočet parametrov kvality vody a o tom, ako môžu satelitné snímky urýchliť proces odhadu v intervaloch definovaných používateľom. Spomínajú sa tu aj predchádzajúce výskumy iných autorov v tejto oblasti. Následne je predstavená nádrž Kamuzu, jej okolie a jej význam pre Malawi. Vysvetľuje význam nádrže a priehrady pre krajinu. Ďalšia časť je venovaná metodológii použitej v rámci štúdie. Sú opísané rôzne typy použitých údajov, ich zdroje a metódy spracovania. Táto časť tiež vysvetľuje kroky podniknuté na integráciu údajov potrebných na získanie výsledkov. V tejto štúdii autori použili údaje zo satelitov Sentinel-2 a Landsat 8 na

odhad rôznych parametrov kvality vody, ako sú chlorofyl-a (Chl-a), celkové nerozpustné látky (TSS), zákal, hĺbka Secchi (SD), cyanobaktérie a farebne rozpustená organická hmota (CDOM). Odhadované hodnoty sa potom porovnali s údajmi in-situ zozbieranými v rieke Lilongwe v Malawi. V časti Výsledky a diskusia sú uvedené zistenia štúdie. Sentinel-2 poskytol presnejšie odhady zákalu a celkového množstva nerozpustených látok v porovnaní s hodnotami odvodenými z Landsat 8. Táto prednosť je spôsobená predovšetkým vyšším priestorovým rozlíšením satelitných snímok Sentinel-2. Súčasťou štúdie sú aj mapy priestorového rozmiestnenia ostatných parametrov v nádrži, ktoré boli vypracované a navzájom porovnané. Parametre odhadnuté z oboch satelitných snímok ukázali silnú koreláciu a konzistentné priestorové rozloženie. Napríklad porovnanie medzi mapami Chl-a a cyanobaktérií preukázalo priamy vzťah, pretože sinice vyžadujú na fotosyntézu chlorofyl. Okrem toho zákal a hĺbka Secchi (SD) vykazovali negatívnu koreláciu, čo je zrejmé z výsledných máp priestorového rozloženia odvodených z údajov Landsat a Sentinel-2. Štúdia tiež dokázala priamu koreláciu medzi celkovým množstvom suspendovaných pevných látok (TSM) a farebne rozpustenou organickou hmotou (CDOM), čo je v súlade so zisteniami iných autorov. Zákal a rozpustený kyslík (DO), ako aj zákal a Chl-a vykazovali negatívne korelácie, ktoré boli pozorované v mapách priestorového rozloženia odvodených z údajov Landsat a Sentinel-2. Okrem toho štúdia vypočítala algoritmus pomeru pásma pomocou satelitných údajov na odhad zákalu a TSM. Tieto odhady sa potom porovnali s údajmi in-situ zozbieranými v rieke Lilongwe v Malawi. Výsledky ukázali pozitívnu koreláciu medzi pomerom pásiem a údajmi in-situ, s hodnotou R2 0,7 pre zákal a 0,9 pre TSM s použitím údajov Sentinel-2. Landsat však poskytol nižšie hodnoty R2 0,6 pre zákal aj TSM. Na základe týchto zistení štúdia dospela k záveru, že údaje zo satelitov Sentinel-2 s vyšším priestorovým rozlíšením 10 metrov možno efektívne použiť na odhad turbidity a TSM. Okrem toho parametre kvality vody odvodené zo satelitu ponúkajú životaschopnú alternatívu k časovo náročnému a nepravidelnému procesu zberu údajov in-situ.

V časti Záver sú zhrnuté hlavné zistenia štúdie. Parametre kvality vody odvodené zo satelitu môžu slúžiť ako budúca alternatíva na urýchlenie tvorby máp kvality vody a uľahčenie včasných opatrení na zabránenie vážneho poškodenia vodných útvarov. Dostupnosť bezplatných satelitných údajov na platformách, ako je Google Earth Engine, spolu s možnosťami cloud computingu ďalej podporuje aplikáciu tejto metodiky na odhadovanie parametrov kvality vody pre akýkoľvek región a to hneď, ako budú satelitné údaje k dispozícii používateľom, zvyčajne však do týždňa.